



LAWRENCE  
LIVERMORE  
NATIONAL  
LABORATORY

# Lithium Ion Solvation and Intercalation at Anode-Electrolyte Interface from First Principles

M. T. Ong, V. Lordi, E. W. Draeger, J. E. Pask

November 3, 2015

251st American Chemical Society National Meeting &  
Exposition  
San Diego, CA, United States  
March 13, 2016 through March 17, 2016

## **Disclaimer**

---

This document was prepared as an account of work sponsored by an agency of the United States government. Neither the United States government nor Lawrence Livermore National Security, LLC, nor any of their employees makes any warranty, expressed or implied, or assumes any legal liability or responsibility for the accuracy, completeness, or usefulness of any information, apparatus, product, or process disclosed, or represents that its use would not infringe privately owned rights. Reference herein to any specific commercial product, process, or service by trade name, trademark, manufacturer, or otherwise does not necessarily constitute or imply its endorsement, recommendation, or favoring by the United States government or Lawrence Livermore National Security, LLC. The views and opinions of authors expressed herein do not necessarily state or reflect those of the United States government or Lawrence Livermore National Security, LLC, and shall not be used for advertising or product endorsement purposes.

# Lithium Ion Solvation and Intercalation at Anode-Electrolyte Interface from First Principles

Mitchell T. Ong,<sup>1</sup> Vincenzo Lordi,<sup>1</sup> Erik W. Draeger,<sup>2</sup> John E. Pask<sup>3</sup>

<sup>1</sup>Materials Science Division, Lawrence Livermore National Laboratory, Livermore, CA 94550

<sup>2</sup>Center for Applied Scientific Computing, Lawrence Livermore National Laboratory, Livermore, CA 94550

<sup>3</sup>Physics Division, Lawrence Livermore National Laboratory, Livermore, CA 94550

## INTRODUCTION

Lithium-ion batteries are a portable alternative energy source that can be used to power modern electronic devices such as mobile phones, laptops and music players. They have also been examined as an alternative to traditional fossil fuels for use in electric and hybrid-electric vehicles. Much research has focused on improving the performance and cycle life of lithium-ion batteries especially since it will require much higher power output for use in these electric vehicles. The performance of a lithium-ion battery is strongly dependent on the mobility of the lithium ions as they move back and forth from the anode and cathode through the electrolyte. Graphite is a common material used for the anode while transition metal oxides are commonly used for the cathode. The electrolyte typically consists of a lithium salt and organic solvent.

Much of the mobility of the lithium ions can be hindered at the interface between the electrode and the electrolyte. Understanding the properties at the electrode/electrolyte interface can be useful in not only reducing the resistance to ion transport, but also improving the cycling life. Li ions must surmount an energy barrier in order to intercalate into the graphite anode. In addition, there usually exists a solid-electrolyte interphase (SEI) that forms due to decomposition of the electrolyte during cycling. The SEI provides a means to keep other decomposition products from reaching the anode while only allowing Li ions to pass through. Still, its presence provides an obstacle for the Li ion to overcome in order to intercalate into the graphite anode.

Li-ion solvation structures and transport properties in bulk non-aqueous electrolytes have been well studied both experimentally<sup>1-5</sup> and theoretically<sup>6-11</sup>. A general consensus among these works indicates lithium prefers 4-fold coordination in tetrahedral fashion with a preference for cyclic carbonates such as ethylene carbonate (EC). EC is a commonly used component for an electrolyte due to its ability to form stable SEI layers in the presence of a graphite anode.<sup>12</sup> It is often mixed with a linear carbonate in order to optimize properties such as the dielectric constant and viscosity, which improves overall transport and battery performance.<sup>12</sup> Impedance measurements have shown evidence that the solvation structure of the Li ion is stripped away before diffusion into the SEI and graphite anode.<sup>1</sup> Experiments by Xu *et al.* have shown that increasing the ratio of EC to linear carbonate results in a higher activation energy barrier for intercalation.<sup>1,13</sup> The authors suggested this was likely due to the stronger dielectric constant of EC, which allows for stronger solvation of the Li ion. Therefore, the larger concentration of EC present will result in a higher energy to de-solvate the Li-ion from its first solvation shell.

In this work, we use first principles molecular dynamics (FPMD) to model the chemistry that takes place at the anode-electrolyte interface in a Li-ion battery without the presence of the SEI layer. We examine the changes in the solvation structure as the proximity of the Li ion approaches the graphite anode. In addition, we examine the kinetics for intercalation of the Li-ion as it inserts into the graphite anode. We compare the energetics for intercalation for different edge terminations of the graphite anode. Finally, we further verify the intercalation energy from our FPMD simulations using the nudged elastic band (NEB)

method to find the minimum energy paths for entry as a function of different edge terminations. We expect that this work will provide insight on how to improve cycling rates for lithium ion batteries by indicating how to optimize ion transport at the anode-electrolyte interface.

## COMPUTATIONAL METHODS

We performed first principles molecular dynamics using density functional theory (DFT) with the projector augmented wave (PAW) method and the Perdew-Burke-Ernzerhof (PBE) generalized gradient approximation exchange-correlation functional, as implemented in the Vienna *ab initio* simulation package (VASP)<sup>14</sup>. A 450 eV plane-wave cutoff was used with Brillouin zone sampling restricted to the  $\Gamma$ -point. All molecular dynamics simulations were performed in the NVT ensemble using a Nose-Hoover thermostat, with a Nose frequency of  $\sim 1000 \text{ cm}^{-1}$  corresponding a period of  $\sim 63 \text{ fs}$  and a time step of 0.5 fs. Each system was equilibrated for 2.5 ps at 330K and then run for another 5 ps to gather statistics. A temperature of 330K was used to mimic an intermediate Li-ion battery operating temperature and to ensure EC was not frozen ( $T_{\text{melt}} = 310\text{K}$ ). A van der Waals dispersion correction<sup>15</sup> by Langreth and Lundqvist (vdW-DF2) was applied to account for dispersion interactions in the system.

A simulation cell was setup consisting of 654 atoms, which include a hydrogen-terminated graphite anode ( $\text{C}_{288}\text{H}_{48}$ ) and 31 EC molecules ( $\text{C}_3\text{H}_4\text{O}_3$ ) and 1  $\text{LiPF}_6$  salt. The density of the electrolyte was  $1.32 \text{ g/cm}^3$  and a Li concentration of 0.46 M. The dimensions of the simulation box were  $38.5\text{\AA} \times 14.79\text{\AA} \times 14.21\text{\AA}$ . The interlayer spacing of the graphite anode was constrained to be  $3.61\text{\AA}$  by fixing the position of one carbon atom in each layer. This is the optimized lattice spacing at this level of theory. Four total layers of graphite were used in the simulation cell with AB stacking. A series of seven constrained molecular dynamics runs were performed where each simulation constrained the Li ion to be a fixed distance from the edge of the graphite anode. The x-position of the Li ion was incremented  $1.93\text{\AA}$  between successive simulations and was held fixed during the dynamics allowing the Li to move in the yz-plane. Solvation structures were characterized with pair correlation functions, calculated using a bin size of  $0.03\text{\AA}$ . Average coordination numbers were computed from the integral of the pair correlation function. An energy profile was obtained by taking the average total energy of each of the seven simulations.

## RESULTS AND DISCUSSION

We have calculated solvation structures of the Li ion at different distances from the edge of the graphite anode using constrained first principles molecular dynamics. Snapshots of solvation structures at different distances from the graphite anode are shown in Fig. 1. We observed that as the Li ion approaches the graphite anode, the number of solvent molecules around the Li ion decreases. This suggests that the Li ion must shed its first solvation shell prior to intercalation into graphite. In addition, we found that the solvent molecules adjust their orientation in order to continue solvating the Li ion. We see that the Li-O-C angle is close to  $90^\circ$  in certain cases where the solvent molecule is located between the Li ion and graphite.

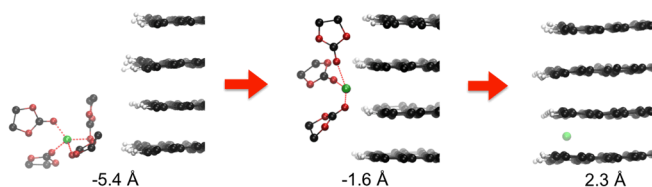


**Figure 1.** Solvation structures at different distances from the graphite anode. Values below snapshots indicate distance of Li ion from graphite edge. Solvent molecules not participating in Li ion solvation are removed for clarity.

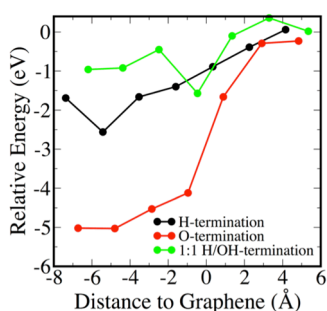


**Figure 2.** Energy profile for constrained FPMD simulations consisting of 31 EC molecules, 1 LiPF<sub>6</sub> and 288 C atom graphite anode with different edge terminations.

We have also approximated the energy barrier for intercalation into the graphite from our constrained FPMD simulations. We compared the energy profile for three different edge terminations: hydrogen-terminated, (carbonyl) oxygen-terminated and 1:1 H/OH-terminated. The energy profile for each of these is given in Fig. 2. We see that the energy profile for the H-terminated and 1:1 H/OH-terminated graphite simulations indicate intercalation barriers that are approximately between 1-2 eV in the presence of organic solvent. However, the oxygen-terminated graphite simulations reveal an energy profile where the barrier is almost 5 eV. Even though we used the average total energy from the FPMD simulations as an approximation to the energy barrier, this is a sizable difference in energetics between the different edge terminations.

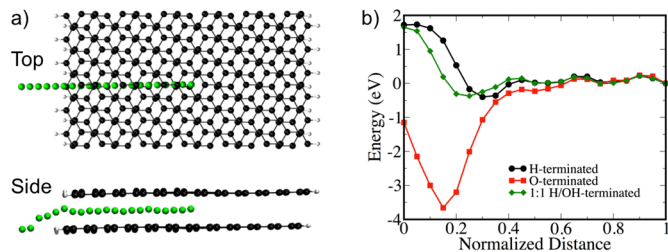


**Figure 3.** (a) Path for Li intercalation into H-terminated graphite using constrained optimization visualized from the top and the side. Li is colored green. (b) Energy profile for constrained optimization pathway for different edge terminations.

In order to confirm the larger intercalation barrier for an oxygen-terminated graphite anode, we performed a series of constrained optimizations for the three edge terminations studied in the FPMD simulations for a graphite bilayer test case. Note that the counter-ion and liquid environment are not included in these calculations. In Fig. 3(a), we show the path of the Li ion as it intercalates into the graphite bilayer for the H-terminated case, while in Fig. 3(b), we show the energy profile that arises from the constrained optimization for each edge termination. We see that from the energy profile that the oxygen-terminated graphite anode does have a larger barrier to intercalation than the other cases. The difference between the oxygen-terminated case and the other two cases is the electrostatic interaction between Li and O that results in a deep minimum prior to entering the bilayer. In addition, we find that the energy profile for all three edge terminations converge as the Li ion moves deeper into the graphite bilayer. This indicates this is the minimum thickness of graphite required to simulate Li in a bulk environment.

## CONCLUSION

We examined the solvation structure of the Li ion as it approaches the graphite anode using constrained first principles molecular dynamics. We found that the coordination number of the solvent

molecules around Li decreases as it moves closer to the graphite suggesting that Li sheds its first solvation shell in order to intercalate into graphite. In addition, we estimate the energy barrier to intercalation using the average total energy for each constraint and found that oxygen-terminated graphite had a larger barrier to intercalation. We verified this observation by running separate constrained optimization simulations on a small bilayer graphite system confirming a larger barrier due to the electrostatic interaction of Li with the oxygen atoms at the edge. Furthermore, our constrained optimization energy profile indicates that the thickness of our bilayer graphite system was the minimum necessary in order to reproduce bulk-like behavior of Li intercalated in graphite. This is valuable information that can be used to design optimal anode/electrolyte systems that improve the cycling rate of lithium ion batteries.

## ACKNOWLEDGEMENTS

This work was performed under the auspices of the U.S. Department of Energy by Lawrence Livermore National Laboratory under Contract DE-AC52-07NA27344. Support for this work was provided through Scientific Discovery through Advanced Computing (SciDAC) program funded by U.S. Department of Energy, Office of Science, Advanced Scientific Computing Research and Basic Energy Sciences. LLNL-PROC-678868

## REFERENCES

- Xu, K.; *J. Phys. Chem. C* **2007**, 111, 7411.
- Bogle, X.; Vazquez, R.; Greenbaum, S.; von Wald Cresce, A.; Xu, K. *J. Phys. Chem. Lett.* **2013**, 4, 1664.
- Han, S.; Yun, S.; Borodin, O.; Seo, D. M.; Sommer, R. D.; Young Jr., V. G.; Henderson, W. A.; *J. Phys. Chem. C* **2015**, 119, 8492.
- Kameda, Y.; Umabayashi, Y.; Takeuchi, M.; Wahab, M. A.; Fukuda, S.; Ishiguro, S.; Sasaki, M.; Amo, Y.; Usuki, T. *J. Phys. Chem. B* **2007**, 111, 6104.
- Nie, M.; Abraham, D. P.; Seo, D. M.; Chen, Y.; Bose, A.; Lucht, B. L.; *J. Phys. Chem. C* **2013**, 117, 25381.
- Borodin, O.; Smith, G. D.; *J. Phys. Chem. B* **2006**, 110, 4971.
- Borodin, O.; Smith, G. D.; *J. Phys. Chem. B* **2009**, 113, 1763.
- Leung, K.; Budzien, J.; *Phys. Chem. Chem. Phys.* **2010**, 12, 6583.
- Ganesh, P.; Jiang, D.; Kent, P. R. C.; *J. Phys. Chem. B* **2011**, 115, 3085.
- Bhatt, M. D.; Cho, M.; Cho, K.; *Modelling Simul. Mater. Sci. Eng.* **2012**, 20, 065004.
- Ong, M. T.; Verners, O.; Draeger, E. W.; van Duin, A. C. T.; Lordi, V.; Pask, J. E.; *J. Phys. Chem. B* **2015**, 119, 535.
- Xu, K.; *Chem. Rev.* **2004**, 104, 4303.
- Xu, K.; *Chem. Rev.* **2014**, 114, 11503.
- Kresse, G.; Furthmüller, J.; *Phys. Rev. B* **1996**, 54, 11169-11186.
- Lee, K.; Murray, E. D.; Kong, L.; Lundqvist, B. I.; Langreth, D. C.; *Phys. Rev. B* **2010**, 82, 081101.